Investigation of Resistivity Impact on AC Losses in Hairpin Conductors

Marco Pastura
Dept. of Engineering Enzo Ferrari
University of Modena and Reggio
Modena, Italy
marco.pastura@unimore.it

Davide Barater
Dept. of Engineering Enzo Ferrari
Università di Modena e Reggio Emilia
Modena, Italy
davide.barater@unimore.it

Stefano Nuzzo
Dept. of Engineering Enzo Ferrari
Università di Modena e Reggio Emilia
Modena, Italy
stefano.nuzzo@unimore.it

Giovanni Franceschini
Dept. of Engineering Enzo Ferrari
Università di Modena e Reggio Emilia
Modena, Italy
giovanni.franceschini@unimore.it

***Abstract*—This work provides an analysis of the impact on AC losses in hairpin conductors, provided by different values of resistivity. Starting from some specific stator geometries, the optimal resistivity which minimizes the AC losses is calculated for each configuration through both analytical and finite element (FE) methods, considering a frequency range typical of automotive applications. Possible applications and conditions where a higher resistivity material, such as aluminum, can be adopted, are discussed. The main sources of discrepancies between the analytical and simulative approach are also discussed.**

Keywords—AC Losses, Resistivity, Aluminum, Hairpin Conductors

I. INTRODUCTION

In the last years the interest for solid bar conductors, especially hairpin conductors, has increased. This trend is evident and in continuous evolution in the automotive sector, but it is gaining attention also in the aerospace field [1]-[3].

Hairpin conductors are basically solid conductors with a nearly rectangular cross section. Thanks to their higher fill factor and an ensuing higher slot thermal conductivity, they can achieve higher torque density values compared to classical stranded round conductors [1]-[4]. In addition, they are more suitable for automated production processes, allowing a reduction of the stator manufacturing costs [5], [6], which is a crucial aspect for a large-scale production.

However, due to their relatively large cross section, hairpin conductors are more sensitive to AC losses. The available literature provides studies on analytical and numerical estimations of AC losses in hairpin windings, and possible solutions to reduce them. Besides the non-uniform current distribution within each conductor due to the high-frequency effects, an important aspect to consider is the uneven distribution of the average current density and, consequently, of losses among conductors located in the same slot. It has been shown that the conductors near the air gap are the most subjected to AC effects (most of all proximity losses due to leakage flux lines) [7]-[9]. For this reason, some research has been focused on how to specifically decrease losses in these more critical conductors, for example with the adoption of variable cross sections or the subdivision of the conductor near the air gap into parallel sub-conductors [10]-[13]. The common denominator is provided by a smaller radial dimension of one or more conductors near the air gap. Although these techniques have shown promising results, their practical implementation has not been verified yet as they present some manufacturing challenges. More practical solutions consist in pushing the conductors towards the slot bottom [7] and increasing the number of conductors per slot, usually with the introduction of some machine parallel paths to allow the machine operation within the voltage limits in all the frequency range [14]-[16]. However, also these techniques have some drawbacks: pushing the conductors towards the slot bottom reduces the fill factor [7] whereas the increase of the number of conductors per slot increases the manufacturing complexity and a suitable transposition becomes mandatory when parallel paths are adopted [14]-[16].

Another interesting option to reduce AC losses in hairpin windings is using conductive materials characterized by a different resistivity than that of the copper. For example, the adoption of aluminium for some of the conductors near the air gap is proposed in [17]. Although the illustrated findings are of interest and promising, the results are provided only for two different frequencies and a single winding configuration. In addition, the adoption of two different conducting materials can provide some challenges in terms of manufacturing.

Considering the above, further investigations on the implementation of non-copper hairpin conductors is needed. On the other hand, the use of copper in high efficiency electrical machines is well consolidated and it relies on its low resistivity. In classical low-voltage machines equipped with random windings, AC losses can be contained thanks to the adoption of parallel strands (or Litz wires in very high-frequency applications [18], [19]), thus, the resistivity of the conductive material should be kept as low as possible to minimize the winding Joule losses (DC losses). However, hairpin conductors cannot be subdivided in strands, hence skin and proximity effects are more prominent. While the DC losses increase with higher values of resistivity, the abovementioned high-frequency phenomena can be mitigated. Therefore, in applications where hairpin windings are adopted and operations up to ≈1 kHz are required, the use of a different material than copper can result in higher

efficiency machines, as well as in additional benefits related to weight and cost considerations.

The aim of this paper is then to investigate the impact of different values of resistivity on active winding Joule losses in hairpin windings. The optimal resistivity values which minimize the losses are provided for 2 study cases, varying both number of conductors and supply frequency. The analysis is performed firstly through the classical analytical approach and then also through FE simulations.

II. Analytical Approach

A. Theoretical Background

As mentioned in Section I, at low-frequency operations as well as at high-frequency operations of machines equipping stranded conductors, the winding resistance should be minimized to mitigate the Joule losses. To such purposes, copper is widely used as it presents a relatively low value of the resistivity. On the other hand, in hairpin windings and at high-frequency operations, the current tends to become distributed within the conductor such that the current density is largest near its surface. The current flows mainly at the "skin" of the conductor, between the outer surface and a level called the skin depth. This is defined in (1), where besides noticing that it depends on the frequency f and the permeability of the material, it can be also observed how the skin depth is proportional to the square root of the resistivity ρ. Therefore, its increase can have positive effects on the AC losses, contrarily to the low-frequency (or high-frequency with suitably stranded conductors) case.

$$\delta = \sqrt{\frac{\rho}{\pi f \mu}} \tag{1}$$

To investigate the effects of resistivity on AC losses, an analytical model is first developed. Only the main formulas are reported here, since the approach has been already described in [7], [10], [15], although with different purposes. Further details about how the formulas can be calculated and all the assumptions can be found in [20].

The analytical approach is based on a simple single slot model and the main hypotheses behind the following formulation are:

- The slot is opened and with a rectangular shape.
- The conductors are rectangular.
- The ferromagnetic material is linear and with an infinite relative permeability (i.e. the magnetic field H is null in the core and saturation is neglected).

Regarding the formulation, the key parameter is provided by the ratio K_r between AC and DC losses (R_{ac}/R_{dc}). Once K_r is estimated, it becomes possible to calculate the AC losses, knowing the conductor dimensions, resistivity and the rms value of the flowing current, by simply applying (2). K_r can be calculated using (3), while the R_{ac}/R_{dc} ratio of the k_{th} slot conductor K_{rk} can be found through (4), starting to count from the slot bottom. In (3) and (4), Z_t is the number of conductors per slot, whereas $\varphi(\varepsilon)$ and $\psi(\varepsilon)$ are defined in (5) and (6) respectively, and are functions of the reduced conductor height ε. This is defined in (7), where h_c is the conductor radial dimension and α is as reported in (8), where b_c and b are the conductor and the slot widths, respectively.

$$P_{AC} = K_r R_{dc} I^2 \tag{2}$$

$$K_r = \varphi(\varepsilon) + \frac{Z_t^2 - 1}{3}\psi(\varepsilon) \tag{3}$$

$$K_{rk} = \varphi(\varepsilon) + k(k-1)\psi(\epsilon) \tag{4}$$

$$\varphi(\varepsilon) = \varepsilon \frac{\sinh(2\varepsilon) + \sin(2\varepsilon)}{\cosh(2\varepsilon) - \cos(2\varepsilon)} \tag{5}$$

$$\psi(\varepsilon) = 2\varepsilon \frac{\sinh(\varepsilon) - \sin(\varepsilon)}{\cosh(\varepsilon) + \cos(\varepsilon)} \tag{6}$$

$$\varepsilon = \alpha \cdot h_c \tag{7}$$

$$\alpha = \sqrt{\pi f \mu_0 \frac{1}{\rho} \frac{b_c}{b}} \tag{8}$$

B. Case Study

The analyses are performed on two different stator structures, which belong to two different permanent magnet assisted synchronous reluctance machines, respectively with 72 and 96 slots. Both the machines have semi-closed slots with the same rectangular shape (i.e. with parallel sides), but characterized by different dimensions. As a consequence, also the conductors' dimensions are different, even when the same number of conductors per slot is considered, allowing to have a larger variety of results. Figure 1 shows an angular sector corresponding to one pole pitch of the 72-slot machine, when the slots comprise 6 conductors. The 96-slot machine has the same structure, but smaller tangential and radial dimension slots, so a lower influence of skin and proximity effects is expected. On the other hand, the rotor structure is unchanged for both the considered cases. In the analytical formulation the influence of the rotor (and of magnets), the core saturation, the tooth shape and the number of slots are inherently neglected, while they are considered in the FE simulations, as it will be shown with more details in the next sections. In fact, as illustrated in section II.A, the analytical approach is based on a single slot model, thus the main parameter which determines the upcoming findings are the conductor dimensions and their number, as well as their resistivity and the supply frequency. The analysis is performed varying these parameters as follows:

- The number of conductors per slot is varied from 2 to 10. Thus, their radial dimension is re-scaled according to their number, keeping the slot depth unchanged and such that they completely fill the slot. Slot depth is equal to 28.3 mm for the 72-slot model and 16.3 mm for the 96-slot one. Their tangential dimension b_c remains fixed, since also the slot width b does not change for a specific case study. It has to be considered that the conductor width is strictly related to the slot width. In addition, as shown by (8), α depends on the square root of b_c/b, so significant variations of this ratio cannot occur. Slot width is b = 4.5 mm and b = 3.4 mm respectively for the 72-slot and 96-slot machine.
- The frequency range is set from 100 Hz to 1 kHz, which is also the operating frequency range of the investigated machines.
- The resistivity boundaries are chosen considering real materials, such that the provided results could have a practical validity. More precisely, the lower bound is

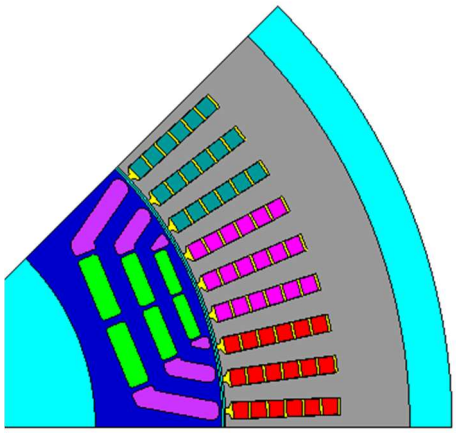

Fig. 1. One pole pitch model of the 72-slot machine, comprising six conductors per slot.

provided by the copper resistivity at a temperature of ≈60 °C, while the upper bound is provided by the aluminium resistivity at ≈180 °C. The obtained results in this specific range can show clearly some important trends.

- The current is supposed to be purely sinusoidal, with a rms value which depends on the number of conductors per slot, such that the imposed magneto motive force (mmf) remains unchanged for each case study.

C. *Analytical Results*

The analytical approach is firstly adopted to estimate the optimal resistivity for each frequency value, which minimizes the losses for a specific geometry. The curves are calculated for each considered number of conductors. For each set of conductors and geometry, the active winding Joule losses have been calculated using (2), by varying ρ and f. From these results it is possible to extrapolate the optimal ρ for each frequency, thus the optimal ρ-f charts. Figures 2 and 3 show the ρ-f charts, respectively for the 72-slot and 96-slot models, taking into consideration the previously mentioned boundaries. With the exception of the case with $n_w = 2$, which is a rather unusual number of conductors per slot in hairpin windings, the curves have the same shape for all the configurations. Below certain frequencies (a few hundreds of Hz for the 72-slot model), the optimal resistivity is provided by the lower limit, meaning that it is worth to adopt a lower resistivity material (copper) to minimize the winding Joule

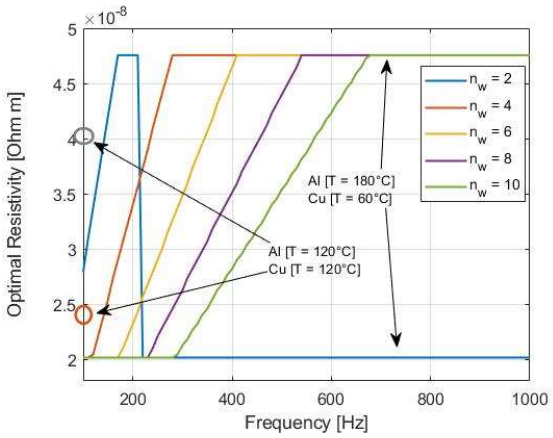

Fig. 2. 72-slot model optimal resistivity as a function of frequency. The number of slot conductors is n_w.

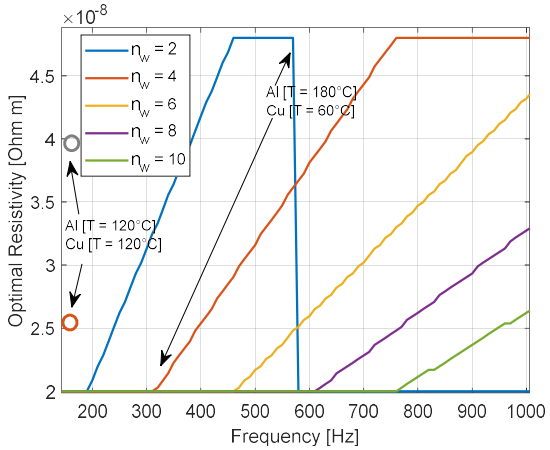

Fig. 3. 96-slot model optimal resistivity as a function of frequency. The number of slot conductors is n_w.

losses. For higher frequency values, the optimum resistivity starts to increase, with the curves assuming the shape of a straight line until the upper boundary is met, meaning that higher resistivity values would be preferable, but not feasible due to practical limits. It can be noticed that increasing the number of conductors per slot reduces the angular coefficient of the straight lines, as well as, the frequency value at which the optimal resistivity starts to increase is shifted towards higher values. This result is predictable since, with a higher n_w, the conductor dimensions are smaller, thus the impact of skin and proximity losses are decreased. This aspect is seen also when the curves obtained for the 72-slot model (Fig. 2) are compared to those obtained for the 96-slot machine (Fig. 3). The 96-slot model can provide the same mmf of the 72-slot model, but it has smaller slots, thus smaller conductors, for a given n_w. Hence, the optimal resistivity straight line curves, are shifted to higher frequencies. Both Fig. 2 and Fig. 3 show also two representative values of resistivity, i.e. those assumed by copper and aluminum at the temperature of 120°C, respectively. These values can help in understanding when one material could be more suitable than the other, or when they can both provide similar results. Basing on the illustrated ρ-f charts, it can be noticed that the 72-slot machine, which features greater conductors, can achieve better results for a wide frequency range with the use of aluminum. On the other hand, for the 96-slot one, the copper would remain the best option for most of the configurations, thanks to presence of thinner conductors which inherently feature lower AC losses in the considered frequency range. In this case, the use of aluminum can be of interest only to reduce the maximum losses, provided at a frequency near the limit of 1 kHz. This would allow to reduce the maximum conductor temperature. However, besides these electromagnetic analyses, it should be considered that the use of aluminum could be preferred to copper in some applications, thanks to its much lower cost and weight. In addition, it has to be considered that the hairpin conductor's radial dimension cannot be reduced below certain practical limits, thus aluminum could have an important potential for high frequency applications above 1 kHz.

III. Comparison Between Analytical and FE Results

A. *Analysis of the Optimal Resistivity*

This section provides a comparison between some of the analytical findings and the results obtained through FE simulations for some specific configurations, such that the

accuracy of the analytical method can be observed and the main sources of error can be spotted. The FE analysis is performed using Flux 2D software. Figure 1 shows one of the simulated models, which corresponds to the PM-assisted synchronous reluctance machine with 72 slots. Since the simulations are carried out considering the 2D aspects only, border and end windings effects are neglected here. In addition, the current angle has been kept fixed for all the cases. The main parameters considered in the FE analyses are the same of the analytical one, i.e. the same frequency and resistivity ranges are investigated. The conductor dimensions, for a fixed n_w, are also the same as well as the slot width and machine active length. The optimal *ρ-f* charts have been calculated following the same procedure. Figures 4-6 show the comparison between analytical and FE results for some specific cases, i.e. 1) 72 slot stator with n_w=6, 2) 72 slot stator with n_w=8 and 3) 96 slot stator with n_w=6. All the other combinations are not provided in this paper as the comparison leads to same results and conclusions. It can be noticed that the trends of the curves are all confirmed with a fair precision. The main difference is provided by the slightly lower angular coefficient and shift towards higher frequencies provided by the FE curves, which means that the analytical formulation may tend to overestimate the AC losses, thus the need of a higher resistivity for a given frequency. However, the difference is not so remarkable, thus the analytical results can be deemed to be rather accurate for this type of studies. Some more considerations can be done observing the figures, where an additional different type of FE solver is used to sport the main source of error. The yellow line curve is obtained with the "steady state AC" (SSAC) FE simulation method. The SSAC assumes all the quantities as sinusoidal and, unlike the transient magnetic solver, can estimate only their average value, as in the analytical formulation. In addition, the SSAC curve is obtained simulating the stator only, as in the analytical case. It can be seen that the SSAC *ρ-f* curve is very similar to the analytical one for Fig.4 and Fig.6, while there is a smaller discrepancy, with respect to the transient method, for Fig.5. The SSAC FE simulations consider the different tooth shape and the core saturation, however Fig. 4 and Fig.6 show that they can provide a low impact on the optimal resistivity and the frequency shift is nearly null with respect to the analytical one. On the other hand, the very similar results provide an additional validation of the analytical formulation. Thus, the comparison with the transient magnetic results, based on the whole 2D machine model, indicates that the rotor can

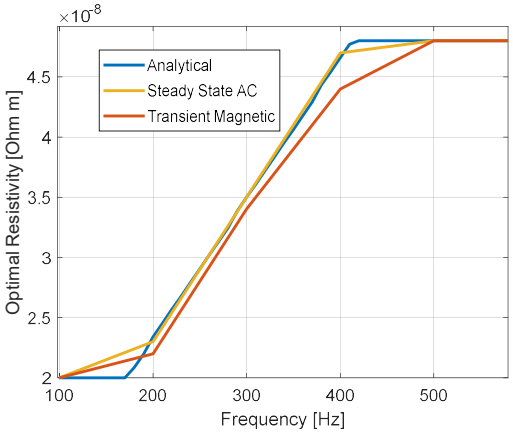

Fig. 4. Optimal *ρ-f* curves for the 72-slot model with six conductors per slot.

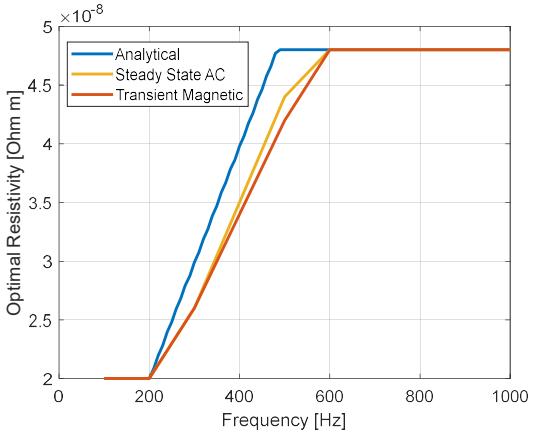

Fig. 5. Optimal ρ-f curves for the 72-slot model with eight conductors per slot.

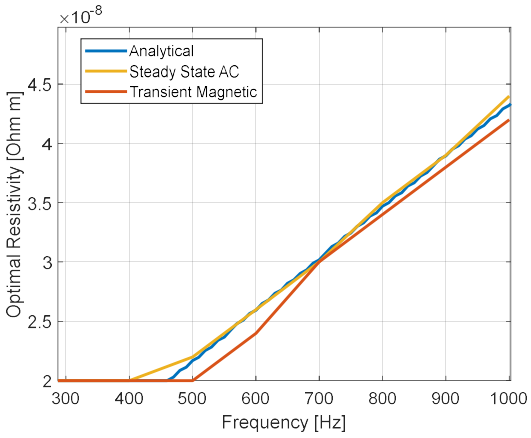

Fig. 6. Optimal ρ-f curves for the 96-slot model with six conductors per slot.

represent the main source of discrepancy between analytical and simulative approaches. Improving the analytical model, taking into consideration only different tooth shape or the local saturation, but neglecting the rotor presence, could not provide significant benefits.

B. Joule Losses Analysis

For the sake of completeness, this section illustrates the quantitative impact on Joule losses given by different resistivity values, such that it is possible to provide stronger conclusions on the possible benefits and drawbacks of using a different material than copper. A comparison between analytical and transient magnetic FE simulations is performed. Figures 7-9 show the active winding Joule losses charts, as a function of frequency, for the same cases considered in the previous sub-section. Although the main trends are confirmed, the analytical formulation tends to overestimate the Joule losses for the 72-slot models, while there is a small underestimation for the 96-slot one. The reason behind this difference is attributable to the effect of the rotor presence and, more precisely, of the saturation and of the rotor internal permanent magnets. On one hand, compared to the rotor-less analytical case, higher losses could be expected due to the magnetic field provided by the magnets as well as the influence of the rotor on the flux lines and the spatial harmonics. However, the core saturation (increased also by the rotor presence) has the effect of decreasing the ferromagnetic material relative permeability in the operating conditions and, consequently, the AC losses.

Thus, two counterbalancing actions are acting on the AC losses, resulting in a small under- or over-estimation. A final important consideration should be done on this aspect. The permanent magnets of the analyzed machines have only the aim of enhancing the output torque, thus their action on the magnetic field, hence on Joule losses, is not predominant. However, for a different machine topology, such as in surface-mounted PM machines, the differences between analytical and FE method could be more significant, thus further studies would be required. Two representative resistivity values have been chosen for the loss comparison. Higher values of resistivity have the effect of flattening the curves, increasing the low frequency losses and decreasing the impact of higher frequencies. It is more evident now that the 96-slot machine does not have particular benefits from the use of aluminum, which could provide lower active Joule losses only above 800 Hz. On the other hand, the 72-slot machine, having larger conductors, can reduce the active Joule losses for a wide range of frequencies thanks to the aluminum. Specifically, the 72-slot machine with eight conductors per slot made of aluminum can provide a comparable amount of losses with respect to the 96-slot machine, thus it could be an interesting lower cost alternative.

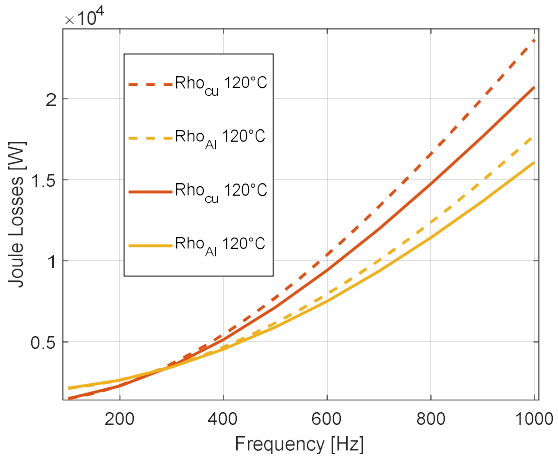

Fig. 7. 72-slot model with six conductors per slot: active Joule losses as a function of frequency - dotted lines: analytical results; solid lines: transient magnetic FE results.

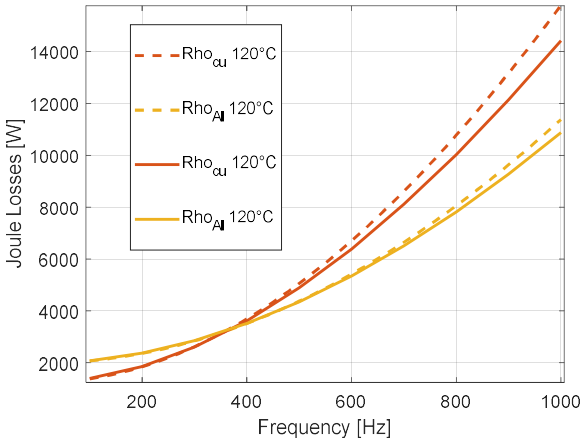

Fig. 8. 72-slot model with eight conductors per slot. active Joule losses as a function of frequency - dotted lines: analytical results; solid lines: transient magnetic FE results.

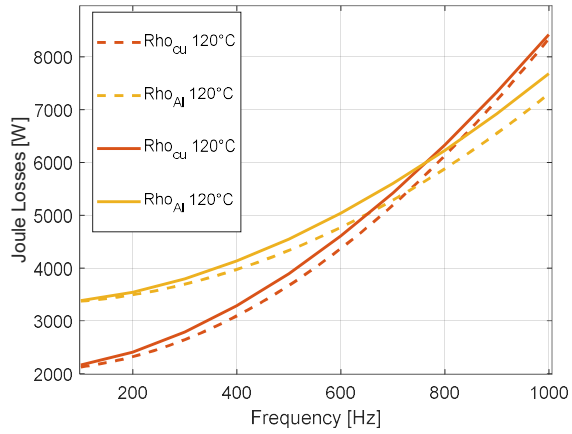

Fig. 9. 96-slot model with six conductors per slot. active Joule losses as a function of frequency - dotted lines: analytical results; solid lines: transient magnetic FE results.

IV. Conclusion

This work presented an analysis on the impact of resistivity on Joule losses in hairpin windings. Two PM-assisted synchronous reluctance machines intended for automotive applications were considered as study cases.

An analytical model was developed to investigate on these aspects. It was shown that, depending on the number of conductors per slot and their dimensions, the aluminum can be beneficial for AC losses reduction. The aluminium can provide positive results from a few hundreds of Hertz for the 72-slot machines, since they have conductors with a greater radial dimension. The 96-slot machine, having smaller cross section conductors, can obtain benefits from aluminium going towards 1 kHz. However, since it is not possible from a practical point of view to reduce the radial dimension below certain thresholds, the aluminium benefits could become important at higher frequencies, representing an interesting solution for all the applications which operate for a significant amount of time above 1 kHz. For applications below 1 kHz, a proper choice of the conductor radial dimension can ensure lower Joule losses with copper.

The analytical findings were validated through FE simulations. The analytical formulation showed an acceptable accuracy in detecting the optimal resistivity which minimizes the AC Joule losses. The main source of discrepancy was attributed to the rotor presence in the models, which however does not have a significant effect in the machine topology analyzed in this paper. However, for different rotor structures, the error of the analytical model could become significant, thus further research would be needed.

Contrarily to classical random windings with stranded conductors, where the copper is always preferable to achieve higher performance, the aluminum could be an interesting solution for reduced AC losses in hairpin windings or at least to achieve similar performance. In addition, the much lower weight and cost of aluminum can make it suitable for a large-scale production.

Acknowledgment

This project has received funding from the Clean Sky 2 Joint Undertaking under the European Union's Horizon 2020 research and innovation program under grant agreement No. 865354.

REFERENCES

[1] Y. Zhao, D. Li, T. Pei and R. Qu, "Overview of the rectangular wire windings AC electrical machine," in *CES Transactions on Electrical Machines and Systems*, vol. 3, no. 2, pp. 160-169, June 2019, doi: 10.30941/CESTEMS.2019.00022.

[2] A. Arzillo *et al*., "Challenges and Future opportunities of Hairpin Technologies," *2020 IEEE 29th International Symposium on Industrial Electronics (ISIE)*, Delft, Netherlands, 2020, pp. 277-282, doi: 10.1109/ISIE45063.2020.9152417.

[3] F. Momen, K. Rahman and Y. Son, "Electrical Propulsion System Design of Chevrolet Bolt Battery Electric Vehicle," in *IEEE Transactions on Industry Applications*, vol. 55, no. 1, pp. 376-384, Jan.-Feb. 2019, doi: 10.1109/TIA.2018.2868280.

[4] A. Reinap, M. Andersson, F. J. Márquez-Fernández, P. Abrahamsson and M. Alaküla, "Performance Estimation of a Traction Machine with Direct Cooled Hairpin Winding," 2019 IEEE Transportation Electrification Conference and Expo (ITEC), Detroit, MI, USA, 2019, pp. 1-6, doi: 10.1109/ITEC.2019.8790545.

[5] F. Wirth, T. Kirgör, J. Hofmann and J. Fleischer, "FE-Based Simulation of Hairpin Shaping Processes for Traction Drives," *2018 8th International Electric Drives Production Conference (EDPC)*, Schweinfurt, Germany, 2018, pp. 1-5, doi: 10.1109/EDPC.2018.8658278.

[6] C. Du-Bar, A. Mann, O. Wallmark and M. Werke, "Comparison of Performance and Manufacturing Aspects of an Insert Winding and a Hairpin Winding for an Automotive Machine Application," 2018 8th International Electric Drives Production Conference (EDPC), Schweinfurt, Germany, 2018, pp. 1-8.

[7] C. Du-Bar and O. Wallmark, "Eddy Current Losses in a Hairpin Winding for an Automotive Application," 2018 XIII International Conference on Electrical Machines (ICEM), Alexandroupoli, 2018, pp. 710-716, doi: 10.1109/ICELMACH.2018.8507265.

[8] S. Xue, M. Michon, M. Popescu and G. Volpe, "Optimisation of Hairpin Winding in Electric Traction Motor Applications," 2021 IEEE International Electric Machines & Drives Conference (IEMDC), 2021, pp. 1-7, doi: 10.1109/IEMDC47953.2021.9449605.

[9] P. H. Mellor, R. Wrobel and N. McNeill, "Investigation of Proximity Losses in a High Speed Brushless Permanent Magnet Motor," Conference Record of the 2006 IEEE Industry Applications Conference Forty-First IAS Annual Meeting, 2006, pp. 1514-1518, doi: 10.1109/IAS.2006.256730.

[10] A. Arzillo et al., "An Analytical Approach for the Design of Innovative Hairpin Winding Layouts," 2020 International Conference on Electrical Machines (ICEM), Gothenburg, 2020, pp. 1534-1539, doi: 10.1109/ICEM49940.2020.9270927.

[11] M. S. Islam, I. Husain, A. Ahmed and A. Sathyan, "Asymmetric Bar Winding for High-Speed Traction Electric Machines," in IEEE Transactions on Transportation Electrification, vol. 6, no. 1, pp. 3-15, March 2020.

[12] S. Nuzzo, D. Barater, C. Gerada and P. Vai, "Hairpin Windings: An Opportunity for Next-Generation E-Motors in Transportation," in IEEE Industrial Electronics Magazine, doi: 10.1109/MIE.2021.3106571.

[13] E. Preci et al., "Segmented Hairpin Topology for Reduced Losses at High Frequency Operations," in IEEE Transactions on Transportation Electrification, doi: 10.1109/TTE.2021.3103821.

[14] G. Berardi, N. Bianchi, "Design guideline of an AC hairpin winding", 2018 XIII International Conference on Electrical Machines (ICEM), pp. 2444-2450, 3.-6. Sept. 2018.

[15] N. Bianchi and G. Berardi, "Analytical Approach to Design Hairpin Windings in High Performance Electric Vehicle Motors," 2018 IEEE Energy Conversion Congress and Exposition (ECCE), Portland, OR, 2018, pp. 4398-4405.

[16] M. Pastura, D. Barater, S. Nuzzo and G. Franceschini, "Multi Three-Phase Hairpin Windings for High-Speed Electrical Machine: Possible Implementations," *2021 IEEE Workshop on Electrical Machines Design, Control and Diagnosis (WEMDCD)*, 2021, pp. 113-118, doi: 10.1109/WEMDCD51469.2021.9425640.

[17] X. Fan, D. Li, R. Qu, C. Wang and J. Li, "Hybrid Rectangular Bar Wave Windings to Minimize Winding Losses of Permanent Magnet Machines for EV/HEVs over a Driving Cycle.," *2018 IEEE International Magnetics Conference (INTERMAG)*, Singapore, 2018, pp. 1-2, doi: 10.1109/INTMAG.2018.8508038.

[18] A. Stadler and C. Gulden, "Copper losses of litz-wire windings due to an air gap," 2013 15th European Conference on Power Electronics and Applications (EPE), 2013, pp. 1-7, doi: 10.1109/EPE.2013.6631820.

[19] A. Bardalai, X. Zhang, T. Zou, D. Gerada, J. Li and C. Gerada, "Comparative Analysis of AC losses with round magnet wire and Litz wire winding of a High – Speed PM Machine," 2019 22nd International Conference on Electrical Machines and Systems (ICEMS), 2019, pp. 1-5, doi: 10.1109/ICEMS.2019.8922173.

[20] J. Pyrhonen, J. Tapani, and V. Hrabovcova,` Design of Rotating Electrical Machines. Chichester, U.K.: Wiley, 2008.